SIMULATION OF LOW REYNOLDS NUMBER ISOTROPIC TURBULENCE INCLUDING THE PASSIVE SCALAR

E. Shirani

Department of Mechanical Engineering
Isfahan University of Technology
Isfahan, Iran

Received April 1987

Abstract Full simulations of homogeneous isotropic turbulence containing a homogeneous passive scalar were made at low Reynolds numbers and various Prandtl numbers. The results show that the spectral behavior of the two fields are quite similar; both fields decay as power–law functions of time. However, the decay exponent is quite dependent on both the Reynolds and Prandtl numbers. The decay exponent of the velocity field seems to fall off somewhat faster as a function of Reynolds number than experiments indicate. The behavior of the velocity derivative skewness is in good agreement with the experimental results but indicates a different trend with Reynolds number than the experiments.

چکیده جریان همگن و ایزوتروپیک مغشوش همراه با یک اسکالر غیر فعال همگن در اعداد رینولدز پایین و اعداد پراندتل مختلف بطور کامل از طریق عددی شبیه‌سازی شده است. نتایج نشان می‌دهد که رفتاراسپکترومهای هر دو میدان جریان و اسکالر کاملا" شبیه یکدیگرند و هر دو میدان بصورت تابع‌نمائی از زمان میرا می‌شوند. البته توان زمان بستگی کامل به اعداد رینولدز و پراندتل جریان دارد. توان زمان در میدان جریان با عدد رینولدز سریعتر از نتایج آزمایش کاهش می‌یابد. رفتار اسکیونس مشتقات سرعت با نتایج آزمایش کاملا" موافقت دارد ولی تغییرات آن با عدد رینولدز روند متفاوتی را در مقایسه با آزمایش از خود نشان می‌دهد.

INTRODUCTION

The concept of isotropic turbulence was introduced by Taylor (1935). Von Karman (1937) introduced the use of tensors in isotropic turbulence, and von Karman and Howarth (1938) studied the statistical theory of turbulence. In 1941, Kolmogoroff suggested that the small-scale components of turbulence are approximately isotropic.

Almost all experiments on isotropic turbulence use rigid, uniform grids to generate the turbulence. The first successful attempt to generate nearly isotropic turbulence was that of Simmon and Salter (1934). They found that at high Reynolds numbers the turbulence far behind a grid is a good approximation to isotropic turbulence. Several other experiments have been carried out, among which that of Comte-Bellot and Corrsin (1971) provides rather complete statistical information. Frenkiel, Klebanoff, and Huang (1979) used both water and air.

The final stage of isotropic turbulence was studied experimentally by Batchelor and Townsend (1950), Tan and Ling (1963), Lee (1965), and Bennett and Corrsin (1978). Also Tavoularis, Bennett, and Corrsin (1979). studied the velocity skewness of isotropic turbulence at small Reynolds numbers.

Numerical simulation of the decay of two-dimensional, isotropic, homogeneous turbulent flows was carried out by Herring, Orszag, Kraichnan, and Fox (1974). The first simulation of three-dimensional, homogeneous, isotropic turbulence was made by Orszag and Patterson (1971). Schumann and Patterson (1975) studied the velocity and pressure fluctuations in isotropic turbulence.

Kwak et al. (1975) and Shaanan et al. (1975) simulated isotropic turbulence by the large eddy simulation technique and obtained very good agreement with the experimental results of Comte-Bellot and Corrsin. Clark et al. (1977) carried out a full simulation at low Reynolds numbers and used it to study subgrid scale modeling.

There is also a series of experiments in heated isotropic turbulence. In all cases, the heating was small enough so that the temperature could be assumed a passive scalar and density variations neglected. The diffusion of heat from a fixed line source in grid-generated, nearly isotropic turbulence was studied experimentally by Schubauer (1935), Collis (1948), Frenkiel (1950), Townsend (1951), Uberoi and Corrsin (1952), Schlien and Corrsin (1974), and Libby (1975). These experiments studied the downstream development of temperature fluctuations and measured statistical properties such as length scales, decay rates, velocity-velocity and velocity-temperature correlations, and spectra.

The fluctuating temperature field in an isotropic turbulence generated by uniformly heated grids was studied by Kistler et al. (1956), Mills and Corrsin (1959), Yeh and van Atta (1973), Sepri (1976), and Warhaft and Lumley (1979) at Taylor microscale Reynolds numbers in the range 60-130. Yeh et al. (1973) carried out an experiment at a relatively low Reynolds number and studied the spectral transfer of the scalar and velocity fields. The results showed that, unlike the decay exponent of the turbulent kinetic energy, the decay exponent of the fluctuating scalar intensity varies considerably from one experiment to another. Antonopoules (1981) simulated homogeneous isotropic turbulence with passive scalar by large eddy simulation and studied the effect of the initial length scales on the decay exponent of the scalar. He concluded that the decay exponent of the scalar is a linear function of the initial length scale ratio and found results in excellent agreement with the experiments. We shall study the effects of Reynolds number and Prandtl number on the decay exponents and concentrate on low Reynolds numbers results.

Non-uniformly heated grids were used by Wiskind (1962) and Venkataramani and Chevray (1978) to generate a uniform temperature gradient in isotropic turbulence Cornelius and Foss (1978) measured the diffusion of particles in isotropic turbulence by a unique method.

METHOD

Since the flows that are simulated in this paper are all at relatively low Reynolds numbers, it is possible to solve the Navier-Stokes equations with no approximations other than the unavoidable numerical ones. Thus, we shall solve the momentum equations

$$\frac{\partial u_i}{\partial t} + \frac{\partial}{\partial x_i} u_i u_j = -\frac{1}{\rho}\frac{\partial p}{\partial} + \nu \frac{\partial^2 u_i}{\partial x_j \partial x_j} \quad (1)$$

together with the continuity equation:

$$\frac{\partial u_i}{\partial x_i} = 0 \quad (2)$$

and the convective-diffusion equation

$$\frac{\partial \theta}{\partial t} + \frac{\partial}{\partial x_j} u_j \theta = D \frac{\partial^2 \theta}{\partial x_i \partial x_i} \quad (3)$$

If we restrict our attention to flows at Taylor microscale Reynolds numbers less than 25, it is sufficient to use a grid of 32 x 32 x 32 mesh points, provided that accurate numerical methods are used. In the calculations presented here, all derivatives were computed

by using Fourier transforms (the pseudospectral method). This method is also perfectly compatible with the periodic boundary conditions that were applied in all three spatial directions.

The second-order Adams-Bashforth method was used for advancing the solution in time. To maintain accuracy, the time step was chosen such that the Courant number based on the maximum velocity was 0.1 or less. The initial levels of the velocity fluctuations were chosen to give the desired Reynolds numbers. The initial spectra of both fields were chosen to have the box shape shown in Figs. 1 and 2; the velocity field was required to satisfy continuity, but both fields were otherwise random. The choice of spectrum was convenient in the absence of experimental guidance, and as shown in the figures, the spectra quickly evolve into realistic ones. This method also avoids the need preselect a spectrum at the low wavenumbers. Since the low wavenumbers have a large influence on the decay of the turbulence, it was felt best to allow the spectrum to develop rather than providing it as input.

With the initial conditions described, the initial stages of the calculations are not realistic representations of turbulent flow fields. For this reason, we ran each simulation until the spectrum developed a realistic shape, the skewness reached a more or less constant approximate value, and the decay curve showed a power law shape.

Runs at Prandtl/Schmidt numbers ($Pr=\nu/D$) of 0.2, 1.0, and 5.0 were made for each Reynolds number. We shall hereafter simply refer to this ratio as the Prandtl number, although it may be interpreted either way.

The calculation was run on the ILLIAC–IV and required 3.2 sec. per time step.

RESULTS

Results for the decay rates, length scales, skewness, and three-dimensional spectra are presented for both hydrodynamic and scalar fields. The list of runs is given in Table 1. We begin by presenting some results for one run, IH32–2. Further results are found in the report by Shirani, (1981).

Table 1. Description of Computer Runs

Simulation	$Re_{\lambda,i}$	$Re_{\lambda,f}$	Pr	λ/λ_θ	n	m	r
IH32–2A	11.00	3.00	0.20	0.634	2.40	3.00	1.25
IH32–3A	22.30	10.00	0.20	0.703	1.70	3.00	1.76
IH32–4A	44.40	22.00	0.20	0.830	1.50	2.90	1.93
IH32–2	11.00	3.00	1.00	1.27	2.40	2.25	0.94
IH32–3	22.30	10.00	1.00	1.23	1.70	1.70	1.00
IH32–4	44.40	22.00	1.00	1.19	1.50	1.61	1.07
IH42–2B	11.00	3.00	5.00	1.68	2.40	0.75	0.31
IH32–3B	22.30	10.00	5.00	1.40	1.70	0.50	0.29
IH32–4D	44.40	22.00	5.00	1.26	1.50	0.34	0.23

A. A Typical Hydrodynamic Field

Figure 1 shows the evolution of the three-dimensional energy spectrum. As stated above, the initial 3–D spectrum is a square wave. It evolves to a realistic low Reynolds number energy spectrum, since the Reynolds number is small, there is no inertial subrange. At low wavenumbers, the spectrum attains a k^4 shape, an expected result. The energy at wavenumbers higher than 2/3 of the maximum wavenumber is set to zero to avoid aliasing and is responsible for the spectral shape seen at t=3.15.

Figure 3 shows the time evolution of the turbulent kinetic energy and its three components. Except in the early "developing" region, the result is a straight line in log-log coordinates. If E(t) is the turbulent kinetic energy at time t, then

$$E(t) = A t^{-n} \qquad (4)$$

where n is the decay exponent. In this particular run, n=2.4.

The decay of the turbulent kinetic energy has been observed in many experiments. It has been shown analytically that the exponent, n, is 2.5 for very low Reynolds numbers. It has been shown both experimentally and analytically that the decay exponent for high Reynolds numbers is 1.20.

The integral length scale, $L_{ij}(r_\ell)$, is defined as twice the distance at which $R_{ij}(r_\ell)$ first reaches 0.1. This differs from the standard definition of the integral length scale, which is the integral of the two-point correlation function. However, since the two-point correlation can have negative values at large r, the standard integral length scale may behave poorly. The time evolution of the integral length scales is shown in Fig. 4.

The Taylor micro-scales are shown in Fig. 5. The Taylor microscale, $\lambda_{ij}(r_\ell)$, is defined as the inverse of the curvture of a two-point correlation at r=0. Both the integral and Taylor micro-scales increase with time. However, the integral length scales increase faster.

B. A Typical Scalar Field

Figure 2 shows the time evolution of the 3–D spectrum of the scalar quantity. It is very similar to the 3–D energy spectrum; in particular, the low wavenumber behavior is k^4. However, the scalar fluctuation spectrum is slightly higher at high wavenumbers. This is also observed experimentally for the flows with Prandtl number close to 1. It suggests that the dissipation in the velocity field is lower than dissipation in the scalar field.

The integral and micro-scales of the scalar quantity are also similar to those for the velocity field. They are shown in Figs. 4 and 5 together with corresponding values for the velocity fields.

The decay of the scalar intensity $<\theta^2>$ with time is shown in Fig. 6. As can be seen, its behavior is similar to that of the turbulent kinetic energy history and can be fit by:

$$<\theta^2> = B t^{-m} \qquad (5)$$

where m is the decay exponent of the scalar and B is a constant. In this particular run, m=2.25, which is within the range obtained from the experimental results. The magnitude of m obtained experimentally varies between 0.87 and 3.0, depending on the initial length scale ratio, λ/λ_θ, and scalar intensity; the Prandtl number was 0.7. There are no experimental results for m at low Reynolds numbers or other Prandtl numbers. This completes the presentation for a particular run. We shall next give synoptic results for the set of runs.

C. Derived Quantities

Nine simulations were made; the parameters of which are given in Table 1. The initial micro and integral-length scale ratios are fixed: $\lambda/\lambda_\theta = 1.23$ and $L/L_\theta = 1.30$. Table 1 shows some statistics for the various runs. In this table, $Re_{\lambda,i}$ and $Re_{\lambda,f}$ are the initial and final Reynolds numbers and r is the ratio of the decay exponents:

$$r = m/n \tag{6}$$

It is also the ratio of characteristic time scales of the velocity and scalar fields:

$$r = \frac{q^2/\epsilon}{<\theta^2>/\epsilon_\theta} \tag{7}$$

where ϵ is the rate of dissipation of kinetic energy and ϵ_θ is half the rate of the dissipation of the scalar intensity,

$$\epsilon_\theta = \frac{1}{2} D <\theta_{,i}\,\theta_{,j}> \tag{8}$$

D. Effects of Reynolds and Prandtl Numbers

In this section, we examine the behavior of the various turbulence statistics as we vary the Reynolds and Prandtl numbers.

1. Microscale Ratio

Figure 7 shows the behavior of the microscale ratio, λ/λ_θ, as a function of Reynolds number for various Prandtl numbers. As can be seen, the microscale ratio increases with Re_λ when $Pr < 1$, and decreases with Re_λ when $Pr > 1$. On the other hand, at high Reynolds numbers, the length scale ratio seems to become independent of Prandtl number. As $Re_\lambda \to 0$, the length scale ratio reaches a constant which depends on the Prandtl number.

2. The Decay Rate

Figure 8 shows the decay exponent of the velocity field, n, vs. Reynolds number. At very low Reynolds numbers, n reaches 2.5. It has been shown analytically (by Batchelor (1953)) that this should be the case. As the Reynolds number increases, the decay exponent n decreases. At high Reynolds numbers, W. C. Reynolds (1976) argues that the asymptotic value should be 1.2. The experimental value of n at high Reynolds number, obtained by Warhaft and Lumley (1978) and Comte-Bellot and Corrsin (1971), is 1.25 ± 0.06. As shown in Fig. 8, the experimental value for n obtained from Tavoularis (2978) is very close to our simulated results. The Bennett and Corrsin (1978) result, however, indicates that the decrease occurs more slowly than what our results indicate. The origin of this discrepancy is not known.

3. Decay Rate Exponent Ratio

The decay exponent ratio, r, defined by Eq. 6, is shown in Fig. 9 as a function of Reynolds number for various Prandtl numbers. As can be seen from this figure, r increases with Reynolds number for $Pr < 1$, and decreases with Reynolds number for $Pr > 1$. At high Reynolds number, r seems to asymptotically reach a constant which depends on Prandtl number. As $Re_\lambda \to 0$, however, it seems that the decay exponent ratio may reach a constant value independent of Prandtl number.

4. The Velocity Derivative of Skewness

Velocity derivative skewness is defined by

$$Sk = <(\partial u_i/\partial x_i)^3> / <(\partial u_i/\partial x_i)^2>^{3/2} \quad \text{(no sum)} \tag{9}$$

Figure 10 shows the skewness. Reynolds

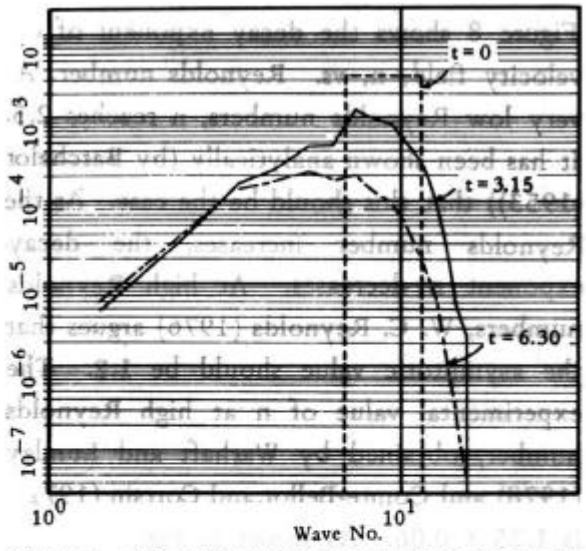

Figure 1. Three-dimensional energy spectra at three different times.

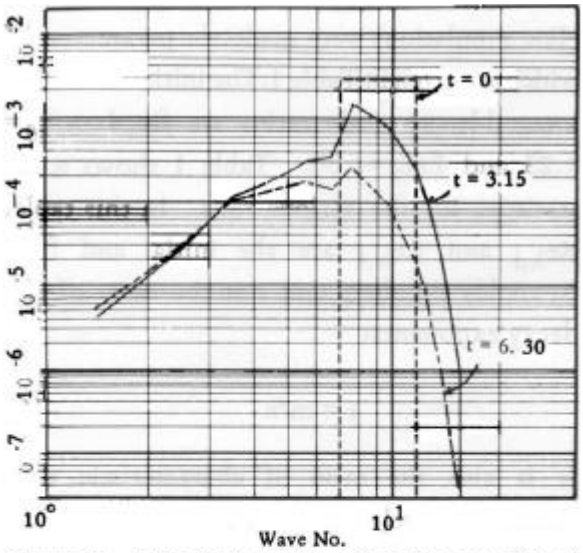

Figure 2. The 3-D spectra of scalar quantity at various times.

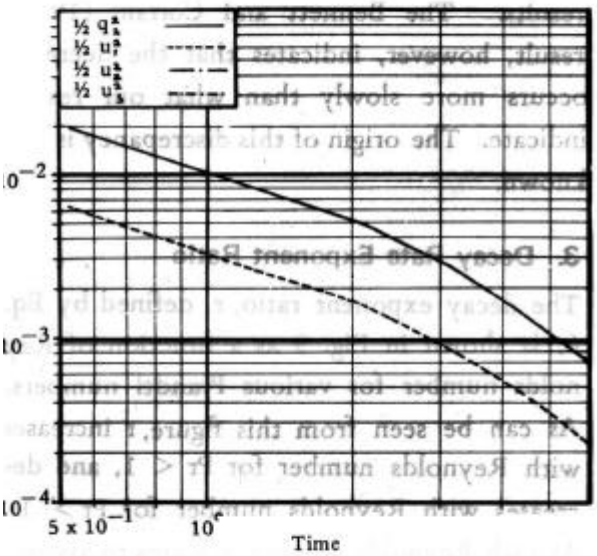

Figure 3. Decay of the turbulent kinetic energy and its components with time.

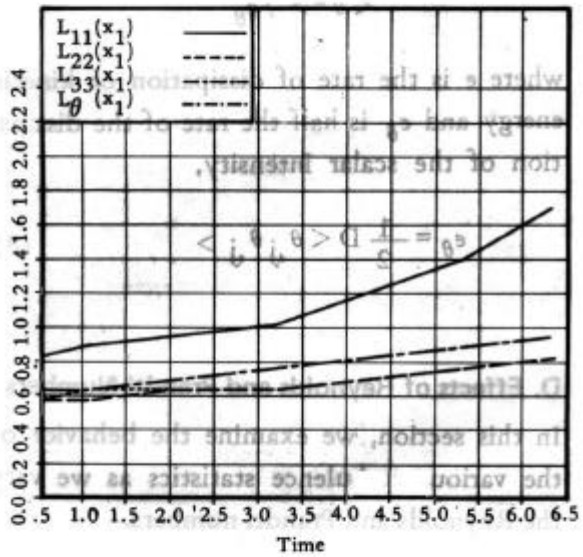

Figure 4. Time evolution of the integral length scales of velocity and scalar fields.

number. The results shown in this figure were obtained from experimental results, the code described above, and a 16 x 16 x 16 mesh point code. As can be seen, skewness has a broad maximum of approximately 0.5 at Re_λ=20. For $Re_\lambda > 20$, skewness decreases, and it seems to reach a constant at about Re_λ=100. At low Reynolds numbers ($Re_\lambda < 20$), the skewness decreases and $Sk \to 0$ as $Re_\lambda \to 0$.

It is interesting to note that the experimental results suggest that $Sk \cong Re_\lambda$ at low Reynolds number, whereas the computational results tend to favor $Sk \cong Re_\lambda$ with p a bit smaller than 0.5.

CONCLUSIONS

We have shown that homogeneous isotropic with and without a passive scalar can be

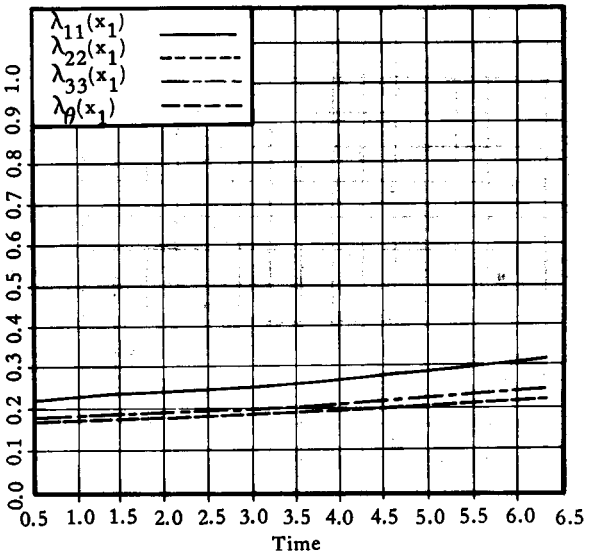

Figure 5. Time evolution of the Taylor microscale of the velocity and scalar fields.

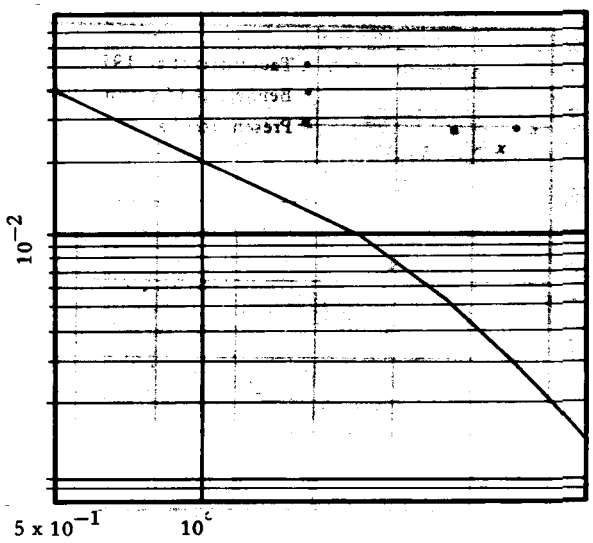

Figure 6. Decay of scalar intensity as a function of time.

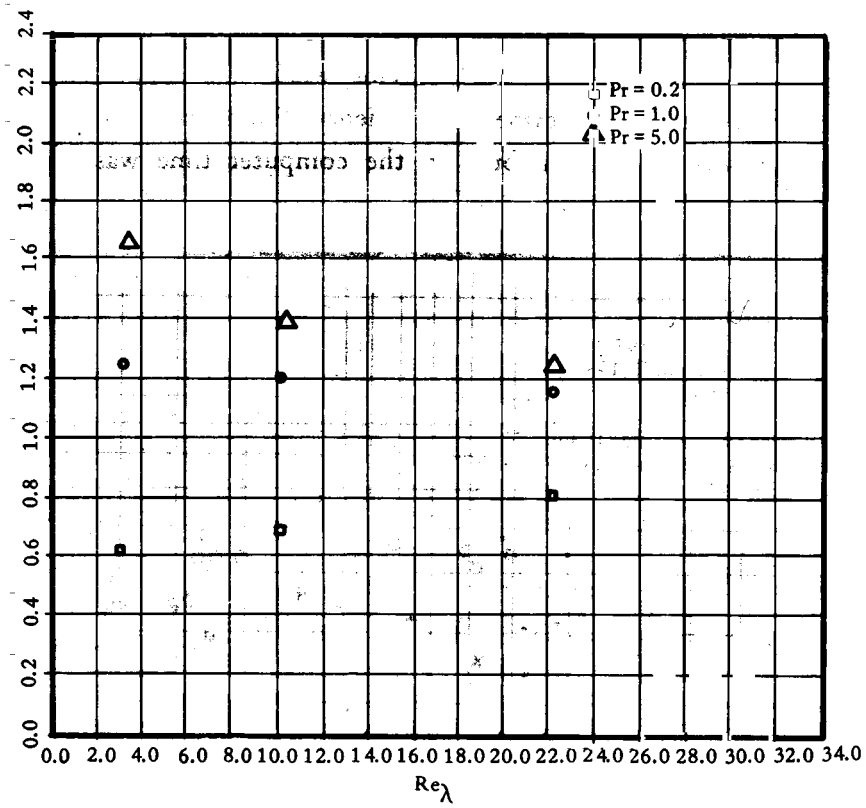

Figure 7. Taylor microscale ratio as a function of Reynolds number for various Prandtl numbers.

simulated accurately. The results are in good agreement with the experiments for all of the quantities that could be compared. New results for the rate of decay of the passive scalar as a function of the Reynolds and Prandtl numbers have been presented. The curve of the decay exponent of the velocity field vs. Reynolds number has been filled in.

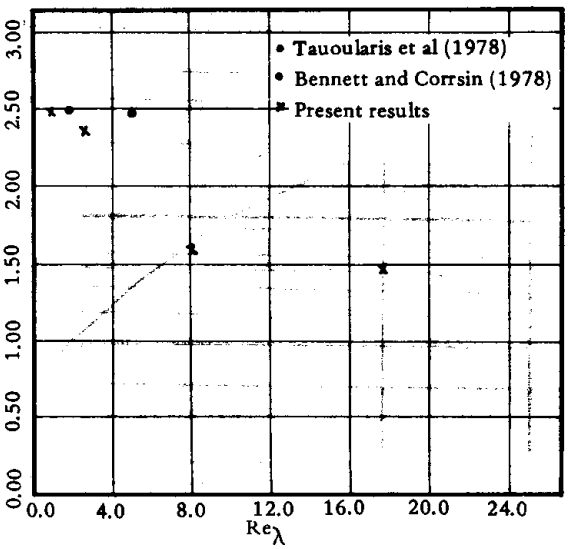

Figure 8. Decay exponent of turbulent kinetic energy as a function of Reynolds number.

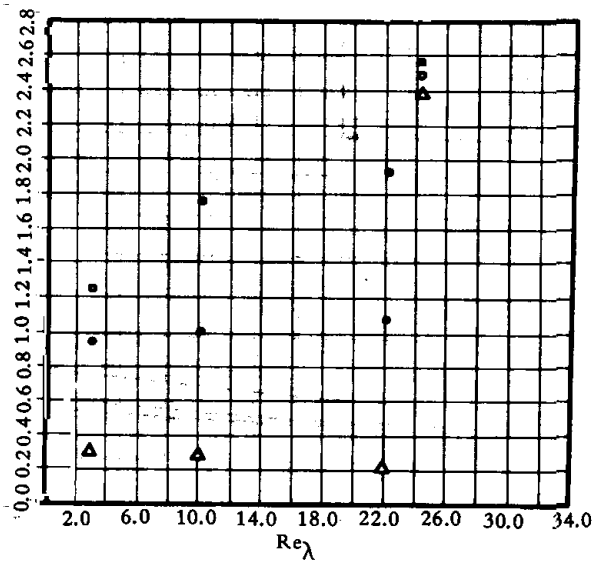

Figure 9. Decay exponent ratio as a function of Reynolds number for various Prandtl numbers.

indicate a different trend as a function of Reynolds number.

The results for the velocity derivative skewness are in good agreement with experiment but

ACKNOWLEDGMENTS

This work was supported by the National Science Foundation under Grant G-17619; the computer time was supplied by NASA-

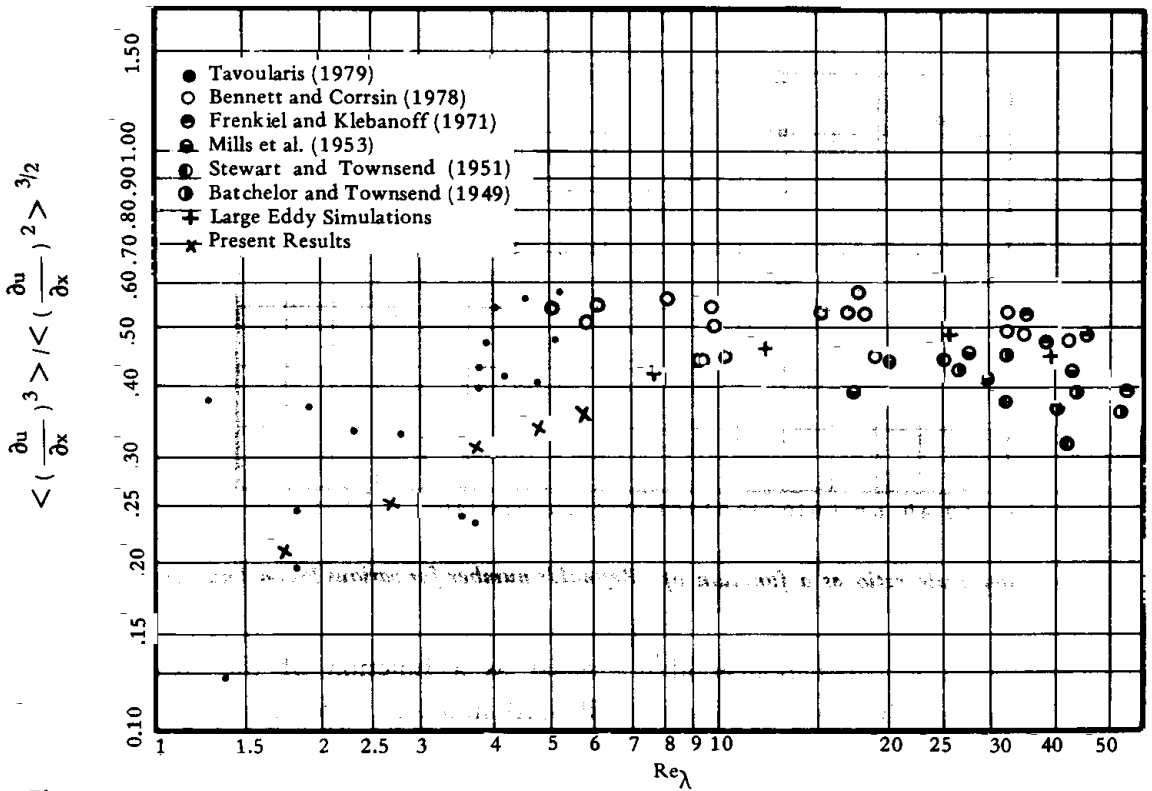

Figure 10. Velocity skewness as a function of Reynolds number.

Ames research Center. The author; would also like to acknowledge the important assistance give by Prof. J. H. Ferziger, Prof. W. C. Reynolds and Drs. R. S. Rogallo, A. Leonard, P. Moin, J. Kim, and W. J. Feiereisen during this work.

REFERENCES

1. Antonopoulos, M., "Large Eddy Simulation of a Passive Scalar in Isotropic Turbulence, "QMC P 6037, Imperial College, London, England (1979).
2. Batchelor, G. K., *The Theory of Homogeneous Turbulence,* Cambridge University Press (1953).
3. Batchelor, G. K., and A. A. Townsend "Decay of Turbulence in the Final Period, *"Proc. Roy. Soc.,* 194, 527 (1948).
4. Bennett, J. C., and S. Corrsin, "Decay of Nearly Isotropic, Grid-Generated Turbulence at Small Reynold: Numbers in a Straight Duct and a Slight Contraction," *Physics of Fluids,* 21, 2129 (1978).
5. Clark, R. A., J. H. Ferziger, and W. C. Reynolds, "Evaluation of Subgrid-Scale Turbulence Models Using a Fully Simulated Turbulent Flow, "Report TF-9, Mech. Engrg. Dept., Stanford Univ. (1977). Also in *J. Fluid Mech.,* 91, 1 (1979).
6. Collis, D. C., "The Diffusion Process in Turbulent Flow," Rept. A55, Aero Div., Australian Council Sci. and Indus. Res. (1948).
7. Comte-Bellot, G., and S. Corrsin, "Simple Eulerian Li Correlation of Full- and Narrow-Band Velocity Signals in Grid-Generated "Isotropic" Turbulence," *J. Fluid Mech.,* 48, 273 (1971).
8. Cornslius, K. C., add J. F. Foss, "An Experimental Study of a Non-Diffusive Scalar Contaminant in the Decaying Turbulence Field on an Enclosed Chamber," Special report to Project SQUID, Mich. State Univ. East Lansing, 1978.
9. Frenkiel, F. N., "On Turbulent Diffusion," Report 1136, 67, Symp. on Turbulence, Naval Ord. Lab (June 1949).
10. Frenkiel, F. N., P. S. Klebanoff, and T. T. Huang, "Grid Turbulence in Air and Water," *Phys. Fluids,* 22, No. 9 (Sept. 1979).
11. Herring, R., S. A. Orszag, R. H. Krachman, and D. G. Fox, "Decay of Two-Dimensional Homogeneous Turbulent Flow," *J. Fluid Mech.,* 66, P3, 417–444 (1974).
12. Karman, T., von, "The Fundamentals of the Statistical Theory of Turbulence," *J. Aero Sci.,* 4, 131 (1937).
13. Karman, T. von, and Howarth, L., "On the Statistical Theory of Isotropic Turbulence," *Proc. Roy. Soc. London A,* 164, 192 (1938).
14. Kistler, A. L., V. O'Brien, and S. Corrsin, "Double and Triple Correlations Behind a Heated Grid," *J. Aeronaut. Sci.,* 23, 96 (1956).
15. Kolmogoroff, A. N., "Energy Dissipation in Locally Isotropic Turbulence." *Duklady AN SSSR,* 32 (1), 19 (1941).
16. Kwak, D., W. C. Reynolds, and J. H. Ferziger, "Three-Dimensional Time-Dependent Computation of Turbulent Flows," Report No. TF-5, Mech. Engrg. Dept., Stanford Univ. (1975).
17. Lee, D. A., "Spectrum of Homogeneous Turbulence in the Final Stage of Decay," *Phys. of Fluids,* 8, 1911 (1965).
18. Mills, R. R., and S. Corrsin, "Effect of Contraction on Turbulence and Temprature Fluctuations Generated , by a Warm Grid," NASA Memo 5–5–59 (1959).
19. Orszag, S. A., and G. S. Patterson, "Numerical Simulation of Three-Dimensional Homogeneous Isotropic Turbulence," *Phys. Rev. Lett.,* 28, Part 2, 76 (1972).
20. Reynolds, W. C., "Computation of Turbulent Flows," *Ann. Rev. Fluid Mech.,* 8, 183–208 (1976).
21. Schubauer, G. B., "A Turbulence Indicator Utilizing the Diffusion of Heat," NACA Rep. 524 (1935).
22. Schumann, U., and G. S. Patterson, "Numerical Study of Pressure and Velocity Fluctuations in Nearly Isotropic Turbulence," *J. Fluid Mech.,* 88, 685 (1978).
23. Sepri, P., "Two-Point Turbulence Measurements Downstream of a Heated Grid," *Phys. of Fluids,* 19, 1876–1884 (1976).
24. Shaanan, S., J. H. Ferziger, and W. C. Reynolds, "Numerical Simulation of Turbulence in the Presence of Shear," Rep. No. TF-6, Mech. Engrg. Dept., Stanford Univ. (1975).
25. Schlien, D. J., and S. Corrsin, "A Measurement of Lagrangian Velocity Autocorrelation in Approximately Isotropic Turbulence," *J. Fuild Mech.,* 62, 255 (1974).
26. Shirani, E., J. H. Ferziger, and W. C. Reynolds, "Mixing of a Passive Scalar in Isotropic and Sheared Homogeneous Turbulence," Report TF-15, Mech. Engrg. Dept., Stanford Univ. (1981).
27. Simmons, L. F. G., and C. Salter, "Experimental Investigation and Analysis of the Velocity Variations in Turbulent Flow," *Proc. Roy. Soc., London A,* 145, 212 (1934).
28. Tan, H. S., and S. C. Ling, "Final Stage Decay of Grid-Product Turbulence," *Phys. Fluids,* 6 (12) (1963).
29. Tavoularis, S., J. C. Bennett, and S. Corrsin, "Velocity-Derivative Skewness in Small Reynolds Number in Nearly Isotropic Turbulent Flow," *J. Fluid Mech.,* 88, Part 1, 63–69 (1978).
30. Taylor, G. I., "Statistical Theory of Turbulence," *Proc. Royal Soc.,* A243, 359 (1935).
31. Townsend, A. A., "The Structure of the Turbulent Boundary Layer," *Proc. Cambridge Phil. Soc.,* 47, 375 (1951).
32. Uberoi, M. S., and S. Corrsin, "Diffusion of Heat from a line Source in Isotropic Turbulence," NACA Tech. Note2710; also NACA Rep. 1142 (1952).
33. Venkataramani, K. S., and R. Chevray, "Total Dispersion of a Scalar Quantity in Turbulent Flow," *Physics of Fluids,* 22, 2284 (1979).
34. Warhaft, Z., and J. L. Lumley, "Study of the Decay of Temperature Fluctuations in Grid-Generated Turbulence," *J. Fluid Mech.,* 88, Part 4, 659–684 (1978).
35. Wiskind, H. K., "A Uniform Gradient Turbulent Transport Expeirment," *J. Geo. Res.,* 67, 3033 (1962).
36. Yeh, I. I., and C. W. Van Atta, "Spectral Transfer of Scalar and Velocity Fields in Heated-Grid Turbulence," *J. Fluid Mech.,* 58, 233 (1973).